Possible promoter sequences for *dmmA*

Consensus sequence in parenthesis

cagatctgtctgtgtagttggggttccccggagcatcctgtagttctgtgtattcatggaattttggaaca
aggattagcttggcaagaagtcgcacttcctctagcagcacaaggttatcgggtagtggctcctgacttat
ttggtcacgggcgctcttctcatttggaaatggtgacttcttatagttcactgacatttttagctcagata
gaccgggtaattcaggaattaccagaccaacctttgttgttagtaggtcattccatgggtgccatgctggc
aactgcgatcatcggaaacgggcctctcacactggatcgtttacgcaccgaggcggcgcgaatccgaccg

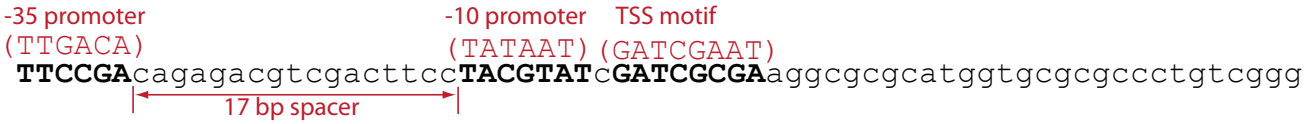

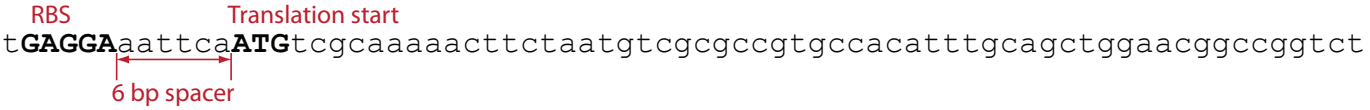

ggttgccgtggcggccggtgtgccggttgcgggccgggcccagtcgcagccgccgcttcaactgccgatct
cgtcggaatttccattcgccaaaaggacggtcgaggtcgaggggggcgacaatcgcctatgttgacgagggc
agtggtcagccagtgctttttctgcacggcaatccgacatcgtcctacctgtggcgcaacatcatcccata
tgtcgtcgctgccgggtatcgcgccgtggcgccggatctgatcggcatgggcgacagcgcgaagcccgaca
tcgaatatcggctgcaggaccacgtggcatatatggatggttttatagacgcgcttggtctcgatgacatg
gtcctggtcatccacgattggggctcggtgatcggcatgcgtcacgcgcggttgaatcccgatcgggtggc
cgctgtcgccttcatggaggcgcttgttccaccggcattgccaatgccaagttacgaggccatggggccgc
aactgggcccgctgtttcgtgatctgcgcacagcggatgtcggcgagaagatggttctcgacggcaatttc
tttgtcgagacgatattgcccgagatgggcgtggtgcggtccctgagcgaagcagagatggcagcctatcg
cgcgccgttcccgacgcgtcagagccggttgcccaccttgcagtggccgcgcgaagtcccgatcggcggcg
agcccgcctttgccgaagccgaggttctgaagaatggcgaatggctgatggcgagcccgataccgaaactg
ctgtttcatgcggaaccgggtgctttggctccgaagccggtggtcgactacctgagcgaaaacgtgcccaa
tcttgaggtccggttcgttggtgctggcacacatttcctgcaggaagatcacccgcacctgatcggtcagg
gcattgccgactggctgcgccgcaacaagccgcagcctcctgacaaaggctgtcaggaggccgatcgtcac
gacctttacgggt

Supplemental Figure 1: Proposed sequence motifs and spacers similar to prokaryotic σ^{70} promoter and ribosome binding sequences upstream of the DmmA coding sequence (1). The -35 and -10 promoter regions, transcription start site (TSS), ribosome binding site (RBS) and translation start site are indicated in bold (consensus in parentheses) and labeled in red.

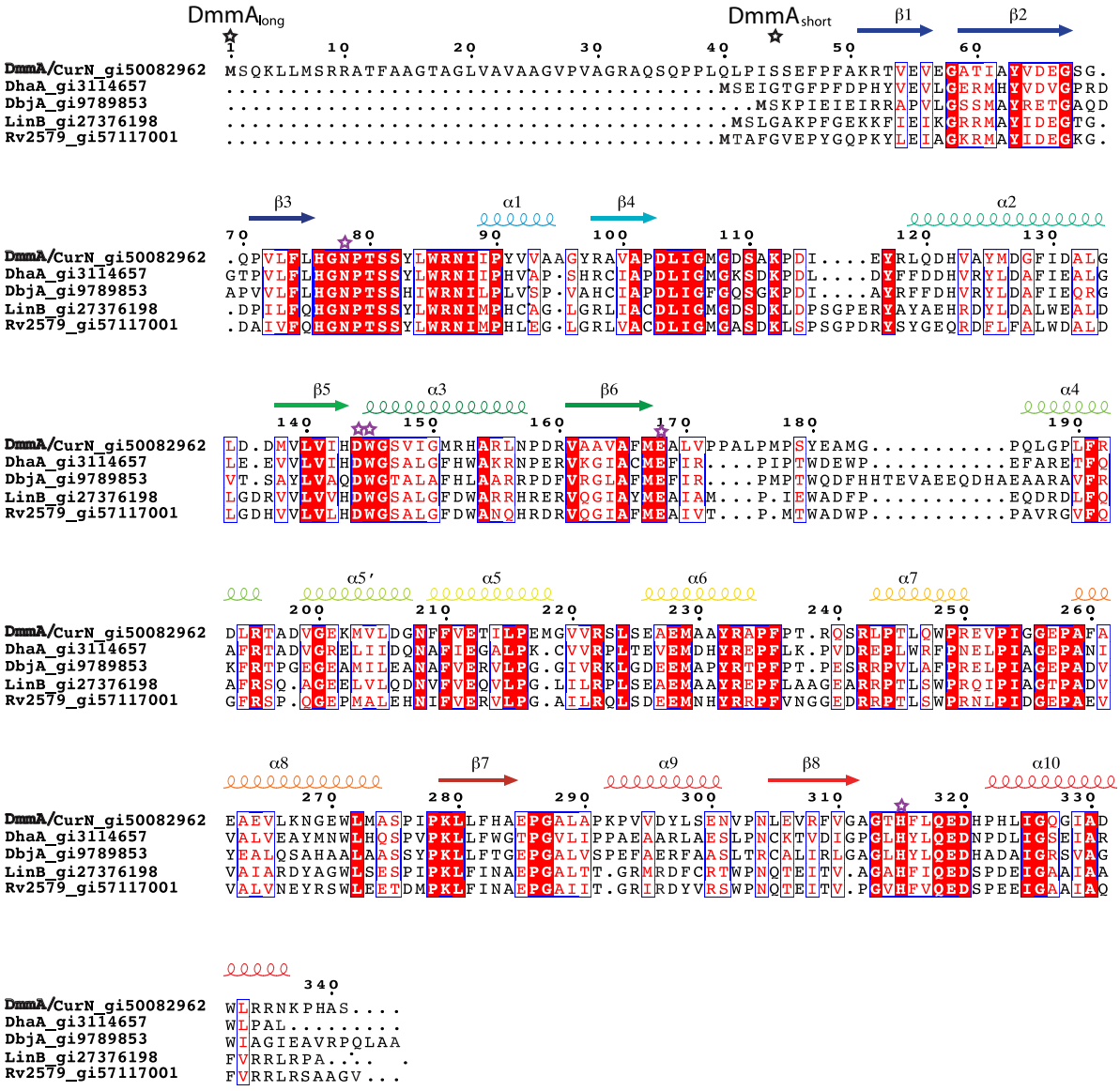

Supplemental Figure 2: Sequence alignment of DmmA to other subfamily II HLDs of known structure. DmmA is aligned with DhaA 1CQW (2), DbjA 3A2M (3), LinB 1IZ8 (4), and Rv2578 2O2I (5). PSI-COFFEE (6) was used to generate the alignment, ESPript (7) to prepare the figure, and the STRIDE server (8) to assign secondary structure. Black stars mark the N-termini of $DmmA_{long}$ and $DmmA_{short}$, and purple stars mark the catalytic pentad.

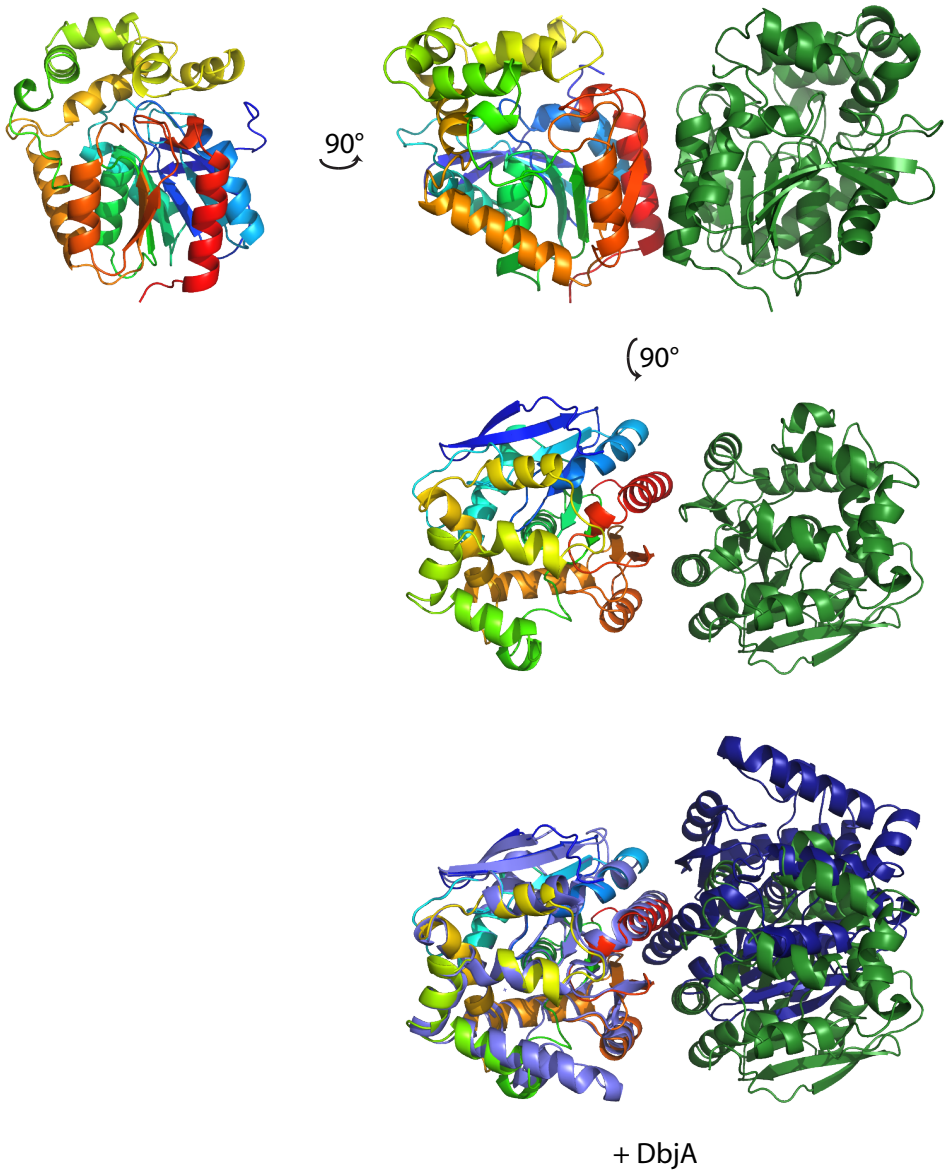

Supplemental Figure 3: Comparison of DbjA dimer interface and DmmA protein-protein contact. DmmA molecules are in rainbow and green and DbjA is in light and dark purple. The same side of DmmA and DbjA forms the contact, but the interactions differ substantially.

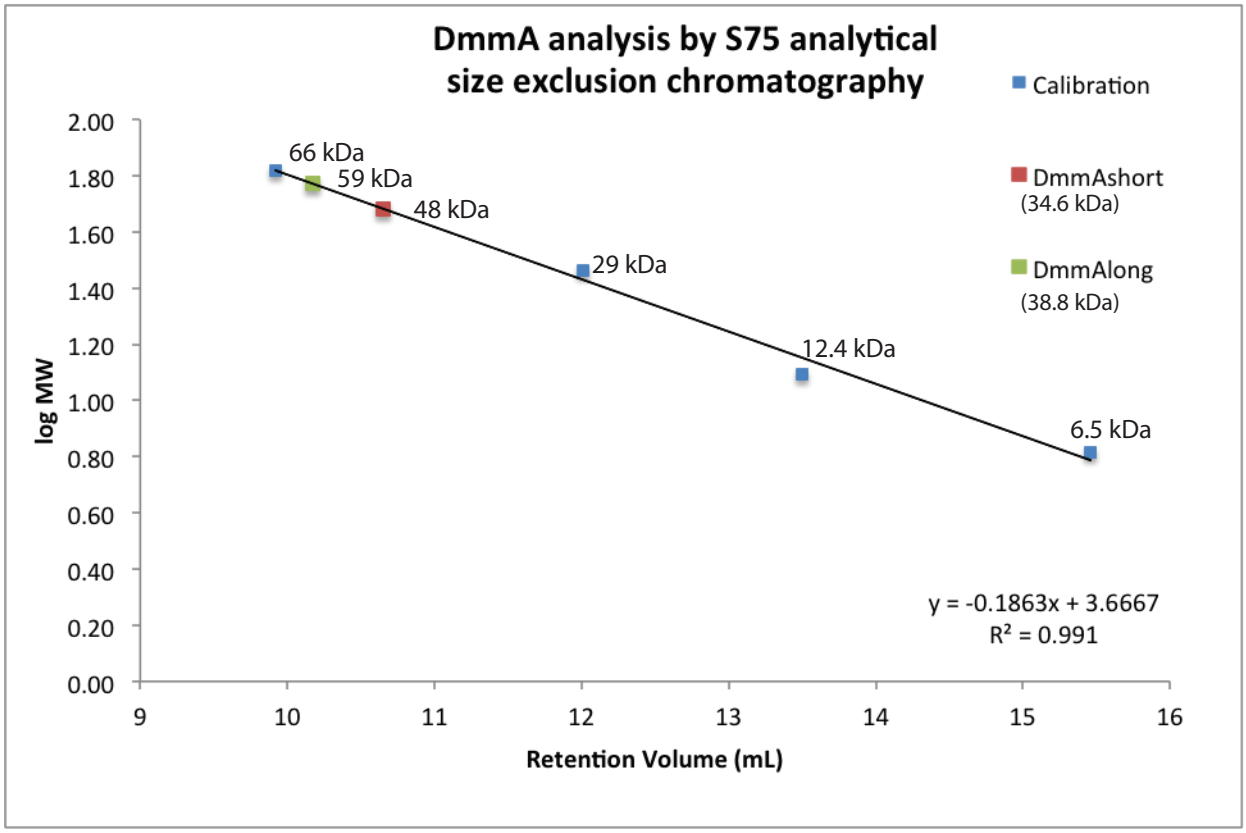

Supplemental Figure 4: Analysis of DmmA oligomeric state by analytical size exclusion. $DmmA_{short}$ and $DmmA_{long}$ (15 mg/mL) were eluted from a Superdex 75 10/300 GL (GE Healthcare) analytical size exclusion column, and compared against standards of known molecular weight and oligomeric state. $DmmA_{long}$ and $DmmA_{short}$ both elute with an apparent molecular weight ($DmmA_{short}$: 48 kDa, $DmmA_{long}$: 59 kDa) between that of the monomer ($DmmA_{short}$: 34.6 kDa, $DmmA_{long}$: 38.8 kDa) and the dimer ($DmmA_{short}$: 69.2 kDa, $DmmA_{long}$: 77.6 kDa). The elution volumes did not shift when the protein concentrations were decreased 4-fold.

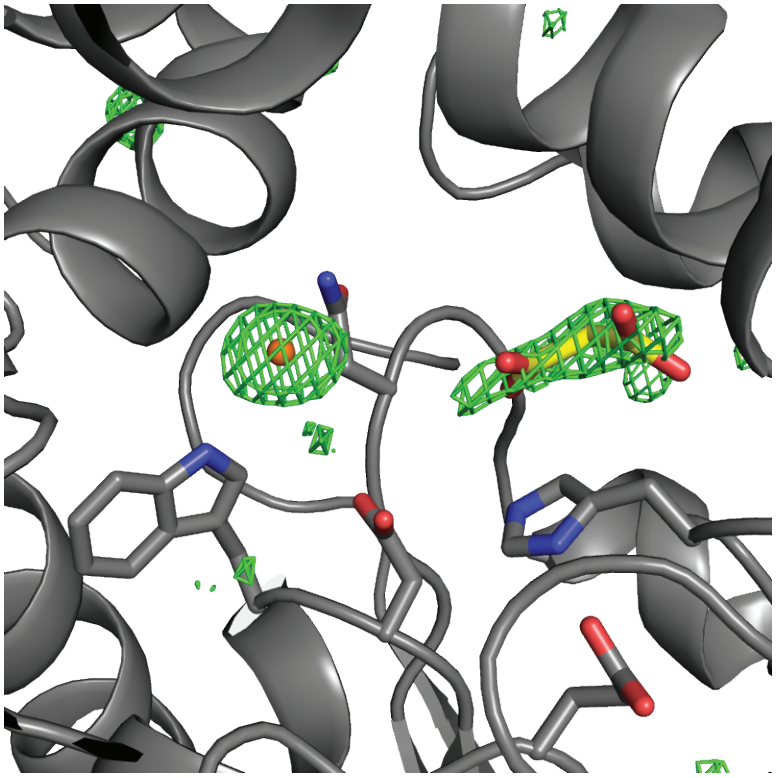

Supplemental Figure 5: Simulated annealing omit map (*Fo*-*Fc*) contoured at 3.5 sigma generated with Cl^- and malonate removed from the atomic model.

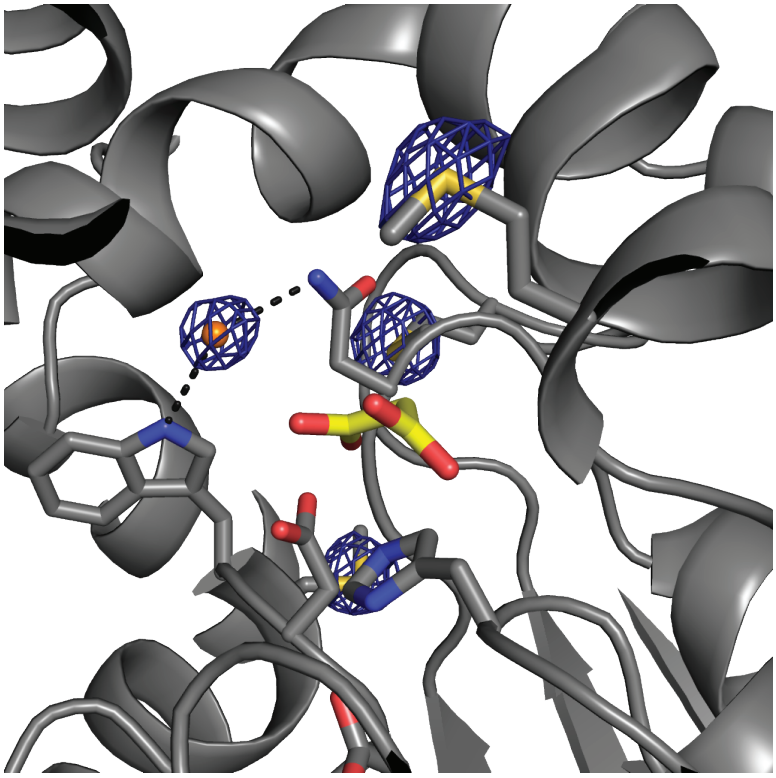

Supplemental Figure 6: Anomalous difference Fourier map using Friedel data collected at the bromine edge. A crystal of SeMet $DmmA_{short}$ was soaked with 1,5-dibromopentane and data were collected at 13.4761 keV. This X-ray energy is 3 eV above the theoretical Br K absorption edge and 800 eV above the Se K edge. The anomalous difference Fourier map contoured at 5.0 sigma shows density for Br^- and for Se atoms in three SeMet side chains.

References:

1. Gordon L, Chervonenkis AY, Gammerman AJ, Shahmuradov IA, Solovyev VV (2003) Sequence alignment kernel for recognition of promoter regions. Bioinformatics 19:1964-1971.

2. Newman J, Peat TS, Richard R, Kan L, Swanson PE, Affholter JA, Holmes IH, Schindler JF, Unkefer CJ, Terwilliger TC (1999) Haloalkane dehalogenases: structure of a Rhodococcus enzyme. Biochemistry 38:16105-16114.

3. Prokop Z, Sato Y, Brezovsky J, Mozga T, Chaloupkova R, Koudelakova T, Jerabek P, Stepankova V, Natsume R, van Leeuwen JG, Janssen DB, Florian J, Nagata Y, Senda T, Damborsky J (2010) Enantioselectivity of haloalkane dehalogenases and its modulation by surface loop engineering. Angew Chem Int Ed Engl 49:6111-6115.

4. Streltsov VA, Prokop Z, Damborsky J, Nagata Y, Oakley A, Wilce MC (2003) Haloalkane dehalogenase LinB from Sphingomonas paucimobilis UT26: X-ray crystallographic studies of dehalogenation of brominated substrates. Biochemistry 42:10104-10112.

5. Mazumdar PA, Hulecki JC, Cherney MM, Garen CR, James MN (2008) X-ray crystal structure of Mycobacterium tuberculosis haloalkane dehalogenase Rv2579. Biochim Biophys Acta 1784:351-362.

6. Di Tommaso P, Moretti S, Xenarios I, Orobitg M, Montanyola A, Chang JM, Taly JF, Notredame C (2011) T-Coffee: a web server for the multiple sequence alignment of protein and RNA sequences using structural information and homology extension. Nucleic Acids Res 39:W13-17.

7. Gouet P, Courcelle E, Stuart DI, Metoz F (1999) ESPript: analysis of multiple sequence alignments in PostScript. Bioinformatics 15:305-308.

8. Heinig M, Frishman D (2004) STRIDE: a web server for secondary structure assignment from known atomic coordinates of proteins. Nucleic Acids Res 32:W500-502.